Structural behavior of secondary-bonded composite joints subjected to Mode II fatigue induced delamination

F P Garpelli[1,2], F M G Ramírez[1], H B Resende[2] and M V Donadon[1]

[1] Divisão de Engenharia Mecânica, ITA – Instituto Tecnológico de Aeronáutica, Praça Marechal Eduardo Gomes, 50, 12228-900, São José dos Campos/SP, Brasil
[2] Laboratório de Estruturas Leves, IPT – Instituto de Pesquisas Tecnológicas, Estrada Dr. Altino Bondensan, 500 – Distrito Eugênio de Melo, 12210-131, São José dos Campos/SP, Brasil

E-mail: felipegarpelli92@yahoo.com.br

Abstract. This paper analyses the Mode II fatigue delamination growth onset for secondary bonded joints compared to co-cured joints. The materials used were composed by two carbon fiber reinforced sub-laminates joined by the secondary bonded and co-cured (without adhesive) methods. Mode II fatigue tests were performed using three-point bending *End Notched Flexure* test setup. The tests were performed under displacement control and a sinusoidal displacement applied at a frequency of 5 Hz with a $R_d = 0.1$, that mean, $\delta_{min} = 0.1\ \delta_{max}$. The main objective of this study was to obtain the strain energy release rate (*SEER*) versus number of cycles (N_f) in order to evaluate the effect of the adhesive on fatigue life of bonded joints. A Closed form solution for 3-ENF setup was used in order to define the displacement amplitudes that were applied in the fatigue test. The results show that the use of adhesive causes a reduction on Mode II fatigue delamination growth onset *SERR* (G_{th}) for secondary-bonded compared to co-cured joints. Finally, a scanning electron microscopy (*SEM*) was used to analyze the fracture surfaces of the Mode II secondary bonded specimens. The fractography images show no crack growth for the specimens tested below or at G_{th} loading levels, which indicated that the value corresponds to the threshold.

1. Introduction

Composite materials been widely employed in the aeronautical industry for the construction of structural components and the aircraft. This trend can be seen through an assessment of the new aircraft produced by today's largest manufacturers, Boeing and Airbus. Boeing's new 787-9 Dreamliner features a set of new technologies of which 50% of the weight is fabricated with composite materials, including fuselage and wings [1]. The Airbus A350XWB was built using 70% of advanced materials, which includes 53% of composites materials and the rest in aluminum and titanium alloys [2]. The properties that can be highlighted are high performance materials with improved mechanical and physical properties. However, composite materials are prone to delamination under cyclic loading, resulting in loss of properties and even component failure. Therefore, it is first necessary to evaluate delamination toughness of the material for the development of damage tolerant structural components [3, 4]. Interlaminar fracture toughness characterization is usually done through interlaminar crack propagations in Mode I (the opening mode), Mode II (the sliding mode) and Mode III (the tearing mode) [3, 4].

In recent years, adhesively bonded joints are being widely used to join composite structures, a method concurrent with traditional mechanical joining [5]. Its advantages over mechanical fastening are: better load transfer, improved fatigue life, damage tolerance, less weight, flexibility and others [6]. For such a methodology to be widely used, in the aeronautical industry, it is necessary further studies to evaluate the behavior of the union, selecting a process that results in good structural performance and reliability in order to obtain parameters that measure the influence of the joint: adhesive, geometry, surface preparation, operating environment, among others. This technology is an alternative that can contribute to reducing the number of parts and final costs, improve the production process and reduced delamination problems [7]. The most commonly used techniques for composite assembly are: co-cured (CC), co-bonded (CB) and secondary-bonded (SB). Secondary-bonding corresponds to the process of joining two cured structural parts with an adhesive [8]. Fernández [9] investigated the 3-ENF procedure in order to evaluate if the results obtained presented reliability for Mode II fatigue test in composite materials using joint technology. It was found that the 3-ENF test is valid and reliable for Mode II fatigue tests on bonded composite joints. So far there is no Mode II standard, therefore in this research these tests will use the 3-ENF configuration, as recommended by Fernández [9].

A deep understanding is needed on the failure modes of bonded joints, since there are several failure modes in adhesive joints, the main ones being: a) delamination of the laminate; b) failure of the interface between the adhesive and the laminate; c) cohesive failure; and d) the combination of them [10, 11]. In this context, the present work aims to evaluate the structural behavior of composite secondary bonded joints subjected to Mode II fatigue induced delamination tested at room temperature ambient in order to obtain the G-N_f curve, following the standard [12], and compare the obtained results with results reported for co-cured joints [13]. A fractography analysis is performed in order to verify the failure mechanism and whether or not there was crack propagation.

2. Material and Methodology

The 3-ENF fatigue tests were performed on unidirectional Torayca® prepreg made of T800 carbon fiber embedded in a 3900-2C epoxy resin. This prepreg also contain thermoplastic polyamide particles on the epoxy resin in order to improve the toughness and consequently reduce the crack propagation [7, 13-16]. The laminates had a $[0^o]_{26}$ layup with a Teflon® film insert in the mid-plane, in order to produce an initial crack for the subsequent interlaminar fatigue tests. The adhesive used for the secondary-bonded (SB) was Loctite® EA 9695 (produced by Henkel®) with a pre-impregnated polyester peel ply to act as thickness controller. The specimens dimensions are: length (L) 175.50 mm, width (B) 20.00 mm, thickness (h) 4.99 mm and initial crack (a_0) 57.50mm. The Flexural Young's modulus (E) was measured in a quasi-static test and the value was 124.12 *GPa*, this result was provided by Brito [7].

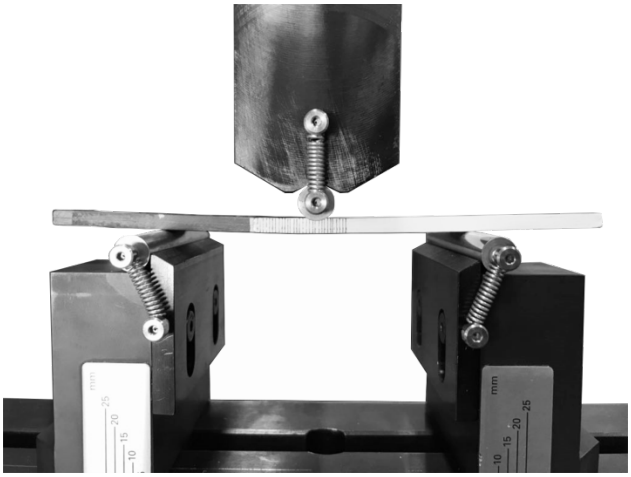

Figure 1. 3-ENF setup fatigue test.

2.1. Mode II fatigue tests

The Mode II fatigue tests were performed on a servo-hydraulic test machine (MTS370.10) with a 15*kN* load cell, at the Lightweight Structures Laboratory (LEL/IPT). The specimens were cycled under displacement control, respecting a sinusoidal function with a displacement ratio of $R_d = 0.1$, that mean, $\delta_{min} = 0.1\ \delta_{max}$, at a 5 *Hz* frequency. A preload of 10 *N* was applied to hold the sample in the test device, as shown in Figure 1.

The criteria used to stop the test was $N_{5\%}$ a (5 % decrease in the maximum cyclic load) as an evidence of crack propagation or N_f equal to 106 cycles that represents the threshold Strain Energy Release Rate (SERR) according to Doker and Marci [17]. The experimental procedure was performed in order to identify the number of cycles to delamination and determining the G - N_f curve.

The displacement values, maximum displacement (δ_{max}), minimum displacement (δ_{min}) and mean displacement (δ_{mean}) required to define the amplitude of the displacement in fatigue cycle tests were determined based on the beam theory. The following equations represent the displacement as function of the load in the middle of the beam, firstly for the linear part, before Eq. (1)) and after (Eq. (2)) the delamination starts. The critical load and displacement can be found from the intersection of Equation (1) and Equation (2) [18].

$$\delta = \frac{P\left(2L^3 + 3{a_0}^3\right)}{12EI} \tag{1}$$

$$\delta = \frac{P}{12EI}\left(2L^3 + \frac{\left(8G_{II}BEI\right)^{\frac{3}{2}}}{\sqrt{3}P^3}\right) \tag{2}$$

where *I* the moment of inertia of the cross-sectional area of the specimen, which is represented by Eq. (3), and G_{IIc} is the Mode II critical strain energy release rate (*SERR*).

$$I = \frac{Bh^3}{12} \tag{3}$$

According to the standard [12], the fatigue Mode I test must be performed cycling between a minimum and maximum displacement at a set frequency. Due to the absence of the standard to 3-ENF fatigue test, the same criteria were adopted to use in Mode II fatigue tests. The maximum cyclic displacement is obtained from an expression which relates the δ_c with an Energy ratio (R_G) to be used in each test, as shown in Equation 4:

$$\left(\frac{\delta_{\max}}{\delta_c}\right)^2 = \frac{G_{IIMax}}{G_{IIc}} \Rightarrow \delta_{\max} = \delta_c\sqrt{\frac{G_{IIMax}}{G_{IIc}}} \Rightarrow \delta_{\max} = \delta_c\sqrt{R_G} \tag{4}$$

Knowing the maximum cyclic load (P_0) acquired at N = 1, it is possible to calculate the maximum *SEER* (G_{IImax}) for different energy (R_G), using Equation 5:

$$G_{IIMax} = \frac{3{P_c}^2{a_0}^2}{8BEI} \tag{5}$$

3. Results and discussion

A typical load displacement curve obtained from quasi-static test using 3-ENF is shown in Figure 2, it is possible to notice that a fairly good correlation between the experimental and analytical results. The critical load and displacement are 2700 *N* and 2.931 *mm*, respectively. The Mode II fracture toughness obtained by Brito [7] were considered, $G_{IImax} = 5.941$ *N/mm*.

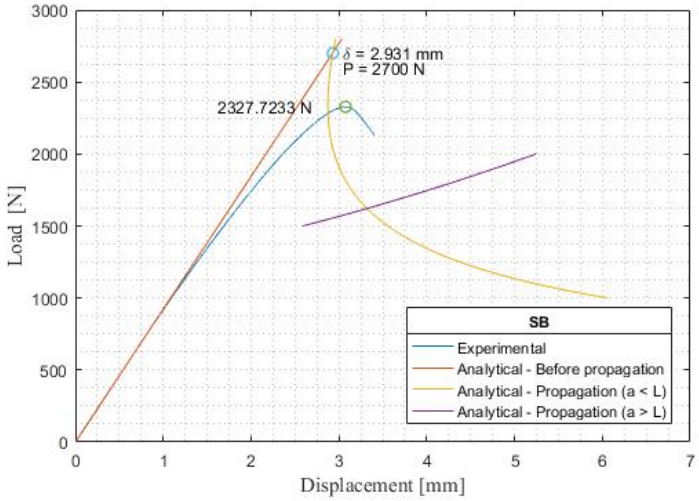

Figure 2. Analytical and experimental load versus displacement curves obtained for Mode II loading.

The results for the fatigue tests of the SB are presented in Figure 3. In all, 14 specimens are tested for energy ratios from 0.95 % to 3.66 %, in order to development the *G-N*$_f$ curve. A trend line was adjusted to obtain an excellent correlation with the experimental points and verify the behavior each sample subjected to different R_G.

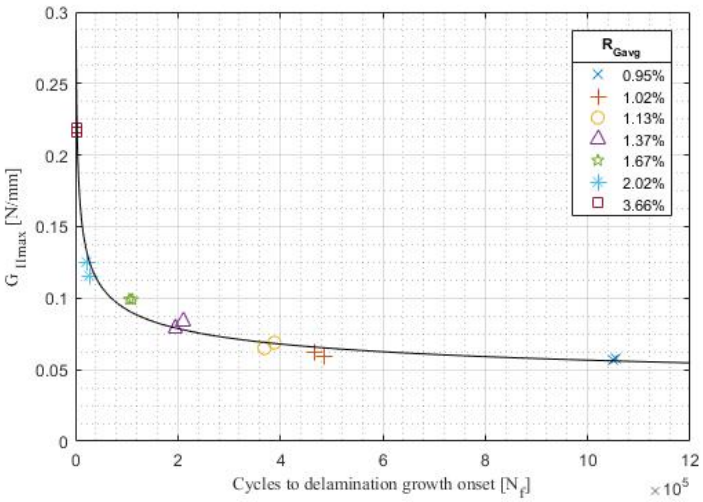

Figure 3. Analytical load versus displacement curve obtained for Mode II loading.

The delamination onset threshold value (G_{th}) under Mode II fatigue tests was found to be 0.95 %, which represent an average value of 0.0567 *N/mm*. Figure 4 represent the comparison of Mode II fatigue curves between SB and CC joint. The fatigue limit under 3-ENF for the CC joint was 8.12 %, corresponding to an average value of G_{th} = 0.0648 *N/mm* for 10^6 cycles [13]. It can be observed that the G_{th} value was higher for the CC joints, followed by the SB.

4. Fractographic analysis

A scanning electron microscope (SEM), model VEGA3 TESCAN, was used in order to verify if there was no crack propagation when reaching 10^6 cycles (threshold) and elucidate the failure modes. Figure 5 presents the fractographic aspects of SB sample tested in RG of 0.95 %. It was observed that no

propagation occurred, only microcracks due to the difference in physical properties between the matrix and the adhesive. The mesh carrier (thickness controller) contributed to crack barrier and act as an obstacle to the crack front. It was confirmed that the sample supported 10^6 cycles without any crack nucleation and the threshold was certified.

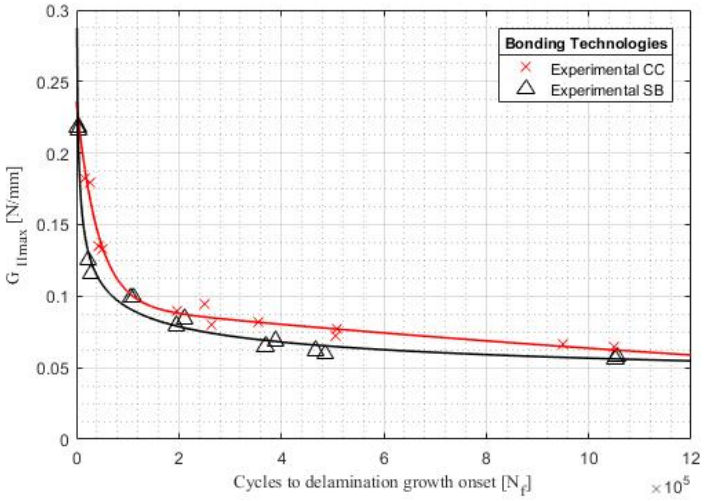

Figure 4. Comparison of Mode II fatigue curves delamination onset.

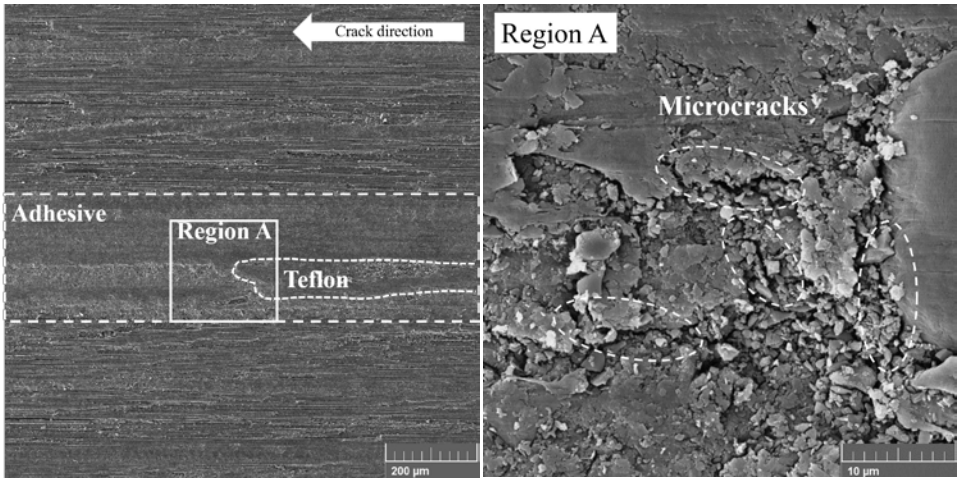

(a) Teflon end. Magnification of 500x. (b) Region A. Magnification of 5kx.

Figure 5: Fracture surface of SB samples tested under Mode II fatigue test.

Figure 6 shows the fracture surface of samples tested under fatigue test. Figure 6a shows that the failure mode was mixed because the initial crack propagation was in the adhesive (cohesive) and propagate to the region between adhesive and matrix (interlaminar failure). The polyamide particles did not act as a crack barrier to the SB sample. Figure 6b shows the polyamide particles in the CC sample. It is possible to note that the polyamide particles have carried out their aim, that accommodates the crack propagation and caused a cohesive failure.

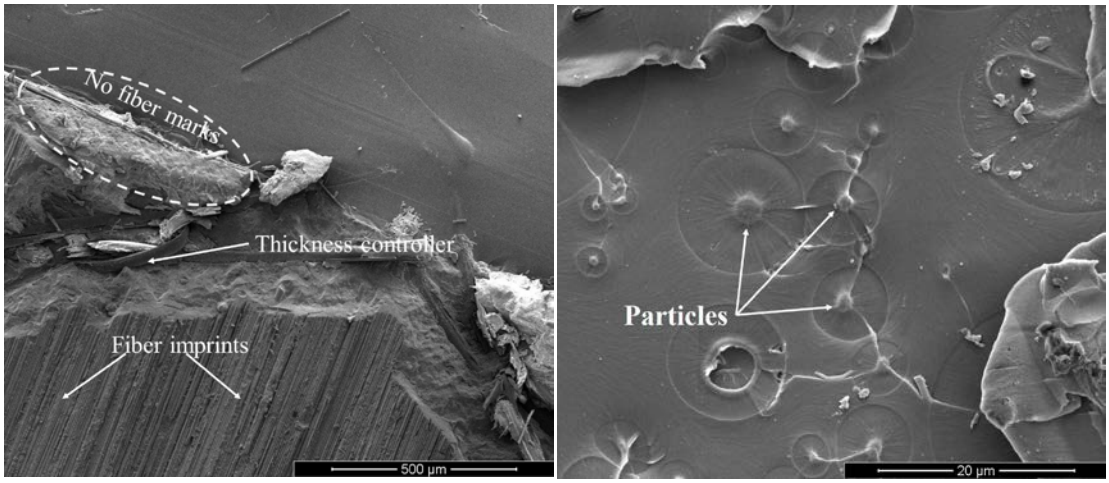

(a) SB. Magnification of 100x. (b) CC. Magnification of 1kx.

Figure 6: Fracture surface of samples tested under fatigue test.

5. Conclusions

The fatigue tests based on Mode II delamination growth onset in secondary-bonded joint at a room temperature condition was explained. The results show that the use of adhesive causes a reduction on Mode II fatigue delamination growth onset SERR (G_{th}) for secondary-bonded because the polyamide particles are not as efficient as in the CC sample. The fatigue threshold value found for Mode II was 0.0567 *N/mm*. Finally, a scanning electron microscopy (SEM) was used to analyze the fracture surfaces. The fractography images show no crack growth for the specimens tested below or at G_{th} loading levels, which indicated that the value corresponds to the threshold.

Acknowledgements

This project is partially supported by the CNPq processes 126346/2016-0, 142761/2016-8, 800319/2016-8, 800392/2016-7 and 300893/2015-9, Capes 1543373, FINEP 0114018300, IPT/FIPT 991914T and FAPESP 2015/16733-2. The authors also acknowledge the LEL-IPT, the Laboratory of Aerospace Structures and Laboratory of Materials and Processes at ITA for providing the infrastructure and equipment needed for the development of this work.

References

[1] BOEING.787 dreamliner advanced composite use, 2017. Available at: www.boeing.com/commercial/787/by-design/advanced-composite-use. Acessed on : Dec, 2017.

[2] AIRBUS.A350, 2017. Available at: www.aircraft.airbus.com/aircraftfamilies/passengeraircraft/- Acessed on : Dec, 2017.

[3] O Al-Khudairi, H Hadavinia, A Waggott, E Lewis, and C Little. Characterising Mode I/Mode II fatigue delamination growth in unidirectional fibre reinforced polymer laminates. *Materials & Design*, **66**:93-102, 2015.

[4] Iréne Maillet, Laurent Michel, Frédéric Souric, and Yves Gourinat. Mode II fatigue delamination growth characterization of a carbon/epoxy laminate at high frequency under vibration loading. *Engineering Fracture Mechanics*, **149**:298-312, 2015.

[5] M D Banea and Lucas F M da Silva. Adhesively bonded joints in composite materials: an overview. *Proceedings of the Institution of Mechanical Engineers, Part L: Journal of Materials: Design and Applications*, **223(1)**:1-18, 2009.

[6] Min-Gyu Song, Jin-Hwe Kweon, Jin-Ho Choi, Jai-Hyun Byun, Min-Hwan Song, Sang-Joon Shin, and Tae-Joo Lee. Effect of manufacturing methods on the shear strength of composite single-lap bonded joints. *Composite Structures*, **92(9):**2194-2202, 2010.

[7] C B G Brito. *Hygrothermal effects on interlaminar fracture toughness of composite joint*s. Master's thesis, Instituto Tecnológico de Aeronáutica, ITA. São José dos Campos /SP. 2017.
[8] A A Baker. *Composite materials for aircraft structures*. AIAA, 2004.
[9] M V C Fernández. *Fracture characterization of composite bonded joints under fatigue loading*. PhD thesis, Universidade do Porto (Portugal), 2013.
[10] S Budhe, M D Banea, S de Barros, and L F M da Silva. An updated review of adhesively bonded joints in composite materials. *International Journal of Adhesion and Adhesives*, **72**:30-42, 2017.
[11] AMERICAN SOCIETY FOR TESTING AND MATERIALS**. D5573-99**: Standard Practice for Classifying Failure Modes in Fiber-Reinforced Plastic FRPM Joints. West Conshohocken, PA: ASTM International, 2012.
[12] AMERICAN SOCIETY FOR TESTING AND MATERIALS. **D6115**: Standard Test Method for Mode I Fatigue Delamination Growth Onset of Unidirectional Fiber-Reinforced Polymer Matrix Composites. West Conshohocken, PA: ASTM, 2011.
[13] F P Garpelli, F M Gonzalez, R Sales, M A Arbelo, M Y Shiino, H B Resende, and M V Donadon. Experimental characterization of Mode II fatigue delamination growth onset in composite joints tested at RTA condition. *Composite Structures (Submitted)*, 2018.
[14] Nobuyuki Odagiri, Hajime Kishi, and Masaki Yamashita. Development of TORAYCA prepreg P2302 carbon fiber reinforced plastic for aircraft primary structural materials. *Advanced Composite Materials*, **5(3)**:249-254, 1996.
[15] Jin Zhang and Bronwyn L Fox. Manufacturing influence on the delamination fracture behavior of the T800H/3900-2 carbon fiber reinforced polymer composites. *Materials and manufacturing processes*, **22(6)**:768-772, 2007.
[16] Jin Zhang, Bronwyn Fox, and Qipeng Guo. Consistent model predictions for isothermal cure kinetics investigation of high performance epoxy prepregs. *Journal of applied polymer science*, **107(4)**:2231-2237, 2008.
[17] H Doker and G Marci. Threshold range and opening stress intensity factor in fatigue. *International journal of fatigue*, **5(4)**:187-191, 1983.
[18] M.V. Donadon and A. Faria. Analysis and design of composite structures – Fracture mechanics applied to composite laminates – Note Class. Technical report, Instituto Tecnógico de Aeronáutica – ITA. São José dos Campos, SP. 02/2016.